



Efficiently Reconfiguring a Connected Swarm of Labeled Robots

Sándor P. Fekete ✉ 

Department of Computer Science, TU Braunschweig, Braunschweig, Germany

Peter Kramer ✉ 

Department of Computer Science, TU Braunschweig, Braunschweig, Germany

Christian Rieck ✉ 

Department of Computer Science, TU Braunschweig, Braunschweig, Germany

Christian Scheffer ✉ 

Faculty of Electrical Engineering and Computer Science, Bochum University of Applied Sciences, Bochum, Germany

Arne Schmidt ✉ 

Department of Computer Science, TU Braunschweig, Braunschweig, Germany

Abstract

When considering motion planning for a swarm of n labeled robots, we need to rearrange a given start configuration into a desired target configuration via a sequence of parallel, continuous, collision-free robot motions. The objective is to reach the new configuration in a minimum amount of time; an important constraint is to keep the swarm connected at all times. Problems of this type have been considered before, with recent notable results achieving *constant stretch* for not necessarily connected reconfiguration: If mapping the start configuration to the target configuration requires a maximum Manhattan distance of d , the total duration of an overall schedule can be bounded to $\mathcal{O}(d)$, which is optimal up to constant factors. However, constant stretch could only be achieved if *disconnected* reconfiguration is allowed, or for scaled configurations (which arise by increasing all dimensions of a given object by the same multiplicative factor) of *unlabeled* robots.

We resolve these major open problems by (1) establishing a lower bound of $\Omega(\sqrt{n})$ for connected, labeled reconfiguration and, most importantly, by (2) proving that for scaled arrangements, constant stretch for connected reconfiguration can be achieved. In addition, we show that (3) it is NP-hard to decide whether a makespan of 2 can be achieved, while it is possible to check in polynomial time whether a makespan of 1 can be achieved.

2012 ACM Subject Classification Theory of computation → Computational geometry; Computing methodologies → Motion path planning

Keywords and phrases Motion planning, parallel motion, bounded stretch, makespan, connectivity, swarm robotics

1 Introduction

Motion planning for sets of objects is a theoretical and practical problem of great importance. A typical task arises from relocating a large collection of agents from a given start into a desired goal configuration, while avoiding collisions between objects or with obstacles. Previous work has largely focused on achieving reconfiguration via sequential schedules, where one robot moves at a time; however, reconfiguring *efficiently* requires reaching the target configuration in a timely or energy-efficient manner, with a natural objective of minimizing the time until completion, called *makespan*. Achieving minimum makespan for reconfiguring a swarm of labeled robots was the subject of the 2021 Computational Geometry Challenge [20]; see [8, 26, 38] for successful contributions.

Exploiting parallelism in a robot swarm to achieve an efficient schedule was studied in recent seminal work by Demaine et al. [12]: Under certain conditions, a labeled set of robots

can be reconfigured with bounded *stretch*, i.e., there is a collision-free motion plan such that the makespan of the schedule remains within a constant of the lower bound that arises from the maximum distance between origin and destination of individual robots; see also the video by Becker et al. [4] that illustrates these results.

A second important aspect for many applications is *connectivity* of the swarm throughout the reconfiguration, because disconnected pieces may not be able to regain connectivity, and also because of small-scale swarm robots (such as catoms in claytronics [22]), which need connectivity for local motion, electric power and communication; see the video by Bourgeois et al. [5]. Connectivity is not necessarily preserved in the schedules by Demaine et al. [12]. In more recent work, Fekete et al. [19] presented an approach that does achieve constant stretch for *unlabeled* swarms of robots for the class of *scaled* arrangements; such arrangements arise by increasing all dimensions of a given object by the same multiplicative factor and have been considered in previous seminal work on self-assembly, often with unbounded or logarithmic scale factors (along the lines of what has been considered in self-assembly [32]). The method by Fekete et al. [19] relies strongly on the exchangeability of indistinguishable robots, which allows a high flexibility in allocating robots to target configurations, which is not present in labeled reconfiguration.

These results have left two major open problems.

1. Can efficient reconfiguration be achieved in a *connected* manner for a swarm of *labeled* robots in a not necessarily scaled arrangement?
2. Is it possible to achieve constant stretch for connected reconfiguration of scaled arrangements of *labeled* objects?

1.1 Our contributions

We resolve both of these open problems.

1. We show that connected reconfiguration of a swarm of n labeled robots may require a stretch factor of at least $\Omega(\sqrt{n})$.
2. On the positive side, we present a framework for achieving *constant* stretch for connected reconfiguration of scaled arrangements of labeled objects.
3. In addition, we show that it is NP-hard even to decide whether a makespan of 2 for labeled connected reconfiguration can be achieved.

1.2 Related work

Algorithmic efforts for Multi-robot coordination date back to the seminal work by Schwartz and Sharir [31] from the 1980s. Efficiently coordinating the motion of many agents arises in a large spectrum of applications, such as air traffic control [10], vehicular traffic networks [18, 30], ground swarm robotics [28, 29], or aerial swarm robotics [7, 37]. In both discrete and geometric variants of the problem, the objects can be *labeled*, *colored* or *unlabeled*. In the *labeled* case, the objects are all distinguishable and each object has its own, uniquely defined target position. In the *colored* case, the objects are partitioned into k groups and each target position can only be covered by an object with the right color; see Solovey and Halperin [33]. In the *unlabeled* case, objects are indistinguishable and target positions can be covered by any object; see Kloder and Hutchinson [24], Turpin et al. [36], Adler et al. [1], and Solovey et al. [35]. On the negative side, Solovey and Halperin [34] prove that the unlabeled multiple-object motion planning problem is PSPACE-hard. Calinescu, Dumitrescu, and Pach [6] consider the sequential reconfiguration of objects lying on vertices of a graph. They give NP-hardness and

inapproximability results for several variants, a 3-approximation algorithm for the unlabeled variant, as well as upper and lower bounds on the number of sequential moves needed.

We already described the work by Demaine et al. [12] for achieving constant stretch for coordinated motion planning, as well as the recent practical CG Challenge 2021 [8, 20, 26, 38]. None of these approaches satisfy the crucial connectivity constraint, which has previously been investigated in terms of decidability and feasibility by Dumitrescu and Pach [15] and Dumitrescu, Suzuki, and Yamashita [17]. Furthermore, these authors have also proposed efficient patterns for fast swarm locomotion in the plane using sequential moves that allow preservation of connectivity [16]. A closely related body of research concerns itself with sequential pivoting moves that require additional space around moving robots, limiting feasibility and reachability of target states, see publications by Akitaya et al. [2, 3].

Very recently, Fekete et al. [19] presented a number of new results for connected, but unlabeled reconfiguration. In addition to complexity results for small makespan, they showed that there is a constant c^* such that for any pair of start and target configurations with a (generalized) *scale* of at least c^* , a schedule with constant stretch can be computed in polynomial time. The involved concept of scale has received considerable attention in self-assembly; achieving constant scale has required special cases or operations. Soloveichik and Winfree [32] showed that the minimal number of distinct tile types necessary to self-assemble a shape, at some scale, can be bounded both above and below in terms of the shape’s Kolmogorov complexity, leading to unbounded scale in general. Demaine et al. [14] showed that allowing to destroy tiles can be exploited to achieve a scale that is only bounded by a logarithmic factor, beating the linear bound without such operations. In a setting of recursive, multi-level *staged* assembly with a logarithmic number of stages (i.e., “hands” for handling subassemblies), Demaine et al. [11] achieved logarithmic scale, and constant scale for more constrained classes of polyomino shapes; this was later improved by Demaine et al. [13] to constant scale for a logarithmic number of stages. More recently, Luchsinger et al. [27] employed repulsive forces between tiles to achieve constant scale in two-handed self-assembly.

1.3 Preliminaries

We consider *robots* at nodes of the (integer) infinite grid $G = (V, E)$, where two nodes are connected if and only if they are in unit distance. A *configuration* is a mapping $C : V \rightarrow \{1, \dots, n, \perp\}$, i.e., each node is mapped injectively to one of the n labeled robots, or to \perp if the node is empty. For a robot ℓ , $C^{-1}(\ell) = (x_\ell, y_\ell)$ refers to its x - and y -coordinate. The configuration C is *connected* if the subgraph $H \subset G$ induced by occupied nodes in C is connected. The *silhouette* of a configuration C is the respective unlabeled configuration, i.e., C without labeling. Unless stated otherwise, we consider labeled connected configurations.

Two configurations *overlap*, if they have at least one occupied position in common. A configuration C is *c-scaled*, if H is the union of $c \times c$ squares of vertices. The *scale* of a configuration C is the maximal c such that C is c -scaled. This corresponds to objects being composed of pixels at a certain resolution; note that this is a generalization of the uniform pixel scaling studied in previous literature (which considers a c -grid-based partition instead of an arbitrary union), so it supersedes that definition and leads to a more general set of results. Two robots are *adjacent* if their positions v_1, v_2 are adjacent, i.e., $\{v_1, v_2\} \in E(H)$.

A robot can move in discrete time steps by changing its location from a grid position v to an adjacent grid position w ; denoted by $v \rightarrow w$. Two moves $v_1 \rightarrow w_1$ and $v_2 \rightarrow w_2$ are *collision-free* if $v_1 \neq v_2$ and $w_1 \neq w_2$. Note that a *swap*, i.e., two moves $v_1 \rightarrow v_2$ and $v_2 \rightarrow v_1$, causes a collision and is not allowed in our model. A *transformation* between two configurations C_1 and C_2 is a set of collision-free moves $\{v \rightarrow w \mid C_1(v) = C_2(w) \neq \perp \wedge |v - w| \leq 1\}$.

Note that a robot is allowed to hold its position. For $M \in \mathbb{N}$, a *schedule* is a sequence $C_1 \rightarrow \dots \rightarrow C_{M+1}$ (also abbreviated as $C_1 \Rightarrow C_{M+1}$) of transformations, with a *makespan* of M . A *stable* schedule $C_1 \Rightarrow_{\chi} C_{M+1}$ uses only connected configurations. In the context of this paper, we use these notations equivalently.

Let C_s and C_t be two connected configurations with equally many robots called *start* and *target configuration*, respectively. The *diameter* d of the pair (C_s, C_t) is the maximal Manhattan distance between a robot's start and target position. The *stretch (factor)* of a schedule is the ratio between its makespan M and the diameter d of (C_s, C_t) .

2 Fixed makespan

Given two labeled configurations, it is easy to see that it can be determined in linear time whether there is a schedule with a makespan of 1 that transforms one into the other: For every robot, check whether its target position is in distance at most 1; furthermore, check that no two robots want to swap their positions. This involves $O(1)$ checks for every robot, thus $O(n)$ checks in total. We obtain the following.

► **Theorem 1.** *It can be decided in $O(n)$ time whether there is a schedule $C_s \Rightarrow_{\chi} C_t$ with makespan 1 for any pair (C_s, C_t) of labeled configurations, with n robots each.*

Proof. Without loss of generality, we assume that the matching between positions from C_s and C_t is perfect. Otherwise, a position is occupied multiple times so no feasible reconfiguration is possible.

To check whether there is a schedule with a makespan of 1, we check for every position $p \in C_s$ whether its matched position $p' \in C_t$ is in distance at most 1; this can be done in $O(1)$ time for each position. Swaps are forbidden, so we also check if any pair of robots need to swap their positions. Because we want to decide whether a schedule with a makespan of 1 exists, this only affects pairs of robots that share their neighborhoods. Thus, this can be done in $O(1)$ time for each position. Because a configuration has n vertices, this takes a total of $O(n)$ time. ◀

On the other hand, Fekete et al. [19] showed that it is already NP-hard to decide whether a schedule with a makespan of 2 can be achieved, if the robot swarm is unlabeled. Due to the desired makespan, the respective target position of every robot is highly restricted. Thus, it is straightforward to provide a suitable labeling of the configurations such that the very same construction shows NP-hardness for the variant of labeled robot swarms.

► **Theorem 2.** *It is NP-hard to decide whether there is a schedule $C_s \Rightarrow_{\chi} C_t$ with makespan 2 for any pair (C_s, C_t) of labeled configurations, with n robots each.*

We use the construction by Fekete et al. [19] that shows NP-hardness for the unlabeled case. Their proof is based on a polynomial-time reduction from the NP-hard problem PLANAR MONOTONE 3SAT [9], which asks to decide the satisfiability of a Boolean 3-CNF formula for which the literals in each clause are either all unnegated or all negated, and the corresponding variable-clause incidence graph is planar. To see that this reduction also yields a feasible construction in the case of identifiable robots, we show that a suitable labeling of the robot swarm exists. Due to the small makespan, the robot's respective target position is highly restricted, as follows.

Proof. Given an instance $\Pi = (C_s, C_t)$ of *unlabeled connected motion planning* that arises via the polynomial-time reduction from an instance of PLANAR MONOTONE 3SAT, see [19].

We construct an instance $\Pi_\ell = (C_s^\ell, C_t^\ell)$ of *labeled connected motion planning* by labeling the positions of the start and the target configuration, such that a schedule with makespan 2 for Π_ℓ is also a schedule for Π .

We create the labeling as follows, using three different colors to indicate occupied positions in the start configuration (red), in the target configuration (dark cyan), and in both configurations (gray). First, the labeling for every gray position is identical in both configurations, C_s^ℓ and C_t^ℓ . A makespan of 2 confines each robot's movement to an area of small radius. Projecting this radius onto any red position in the clause/auxiliary gadgets, the bridges and the variable gadgets of Π , leaves only a single dark cyan position in range. These red-cyan pairs get the same labeling in C_s^ℓ and C_t^ℓ , respectively. In the separation gadget there is a red position with two possible dark cyan positions in range, see Figure 1. However, only one of these admits a feasible matching of all positions, i.e., the labeling is also unique in these separation gadgets.

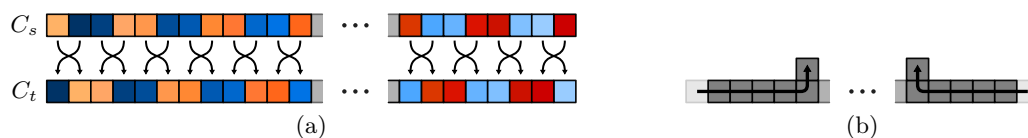


■ **Figure 1** For the separation gadget, there is only one feasible matching. The dotted lines indicate the range of motion for the central red robot.

Due to the unique labeling within each gadget, it is straightforward to observe that there is a schedule with a makespan of 2 (implying that there are two different schedules for the variable gadget due to the two possible assignments) realizing the reconfiguration given by the labeling. Because the labeling is unique, the schedule for Π_ℓ yields a schedule for Π . Hence, we conclude that the labeled variant is at least as hard as the unlabeled one. ◀

3 Lower bound on stretch factor

We show a lower bound of $\Omega(\sqrt{n})$ on the stretch factor. For this, we consider the pair of configurations (C_s, C_t) shown in Figure 2(a), both consisting of n robots. The difference between both configurations is that adjacent robots need to swap their positions. Thus, the diameter of (C_s, C_t) is $d = 1$. Because swaps are not allowed within the underlying model, some robots have to move orthogonally.



■ **Figure 2** Pairs of robots must swap their positions (a), using moves that involve all robots (b).

A single transformation allows for at most 2 robots to move orthogonally without disconnecting the configuration. A crucial insight is that each of these robots can realize at most one swap in parallel.

► **Theorem 3.** *There are pairs of labeled configurations C_s and C_t , each with n vertices, so that every schedule $C_s \Rightarrow_\chi C_t$ has a stretch factor of at least $\Omega(\sqrt{n})$.*

Proof. Consider a start configuration consisting of n robots arranged in a straight line, and a target configuration that arises by swapping each adjacent pair of robots. This pair of configurations has a diameter of $d = 1$, with a total of $n/2$ swaps. A minimum makespan may be achieved by rearranging adjacent robots in parallel. This parallelism is limited by the rate at which robots can move orthogonally to the linear arrangement, see Figure 2(b).

For some $\lambda \in \{0, \dots, \lceil n/2 \rceil\}$, the process of freeing 2λ robots out of the line such that they can navigate along the configuration freely would take a total of λ transformation steps. With each free robot we can reduce the number of swaps of the remaining line by 1 in a constant number of steps. Therefore, realizing all swaps takes at least $\Omega(n/\lambda)$ transformation steps, resulting in a total makespan of $\Omega(\lambda + n/\lambda)$. This is asymptotically minimal for $\lambda = \sqrt{n}$, resulting in a makespan of at least $\Omega(\sqrt{n})$. Because of the diameter $d = 1$, this implies that any schedule has stretch at least $\Omega(\sqrt{n})$. ◀

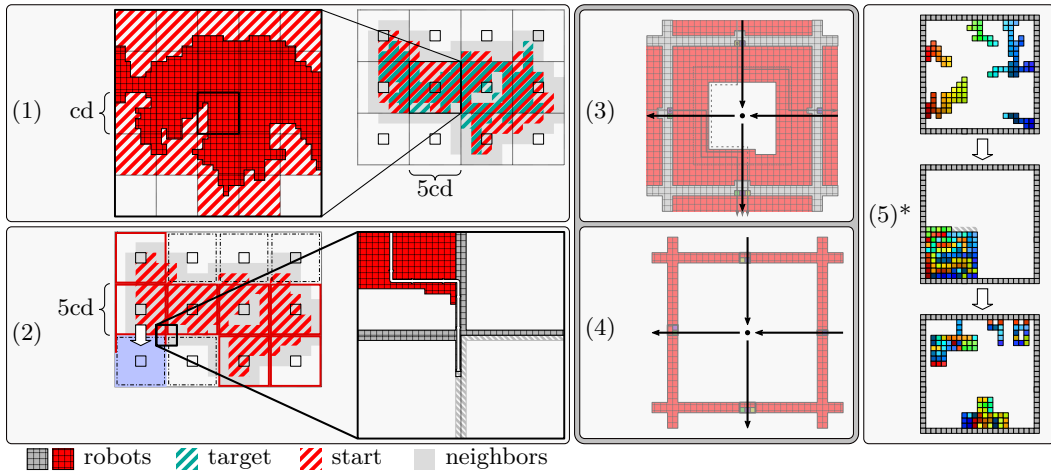
4 Schedules of constant stretch

In this section, we describe an approach to determine stable schedules with constant stretch for labeled configurations of sufficient scale. In particular, we show the following result.

► **Theorem 4.** *There is a constant c^* such that for any pair (C_s, C_t) of labeled configurations with n robots each and scale of at least c^* , there exists a constant stretch schedule $C_s \Rightarrow_{\chi} C_t$.*

4.1 Overview of the algorithm

Our approach works in different phases; Figure 3 provides an overview. Based on (1) pre-processing steps (Section 4.4) in which we determine the scale c and the diameter d of the configurations, we (2) build a tile-based scaffolding structure (Section 4.5) that guarantees connectivity during the reconfiguration. Then the actual reconfiguration (3+4) consists of shifting robots between adjacent tiles based on flow computations (Sections 4.6–4.9), and (5) reconfiguring tiles in parallel (Sections 4.3 and 4.10). Finally, the deconstruction of the scaffold yields the target configuration.



■ **Figure 3** Overview of our algorithm. *Note that ideas of Phase (5) are also used as a subroutine in Phases (2) to (4).

On a technical level, the phases can be summarized as follows.

- Phase (1) Preprocessing:** Compute scale c , diameter d , a tiling \mathcal{T}_1 of the grid into squares of size $cd \times cd$, and a larger tiling \mathcal{T}_5 covering all non-empty tiles of \mathcal{T}_1 .
- Phase (2) Scaffold construction:** Construct a scaffold along the edges of \mathcal{T}_5 , resulting in a tiled configuration, guaranteeing connectivity during reconfiguration.
- Phase (3) Interior flow:** Create a flow graph $G_{\mathcal{T}_5}$ to model the movement of interior (non-scaffold) robots between adjacent tiles of \mathcal{T}_5 . Convert the flow into a series of moves, placing all interior robots in their target tiles.
- Phase (4) Boundary flow:** Analogously to Phase (3), create a flow for the robots that were used to construct a scaffold in Phase (2). Afterwards, move all of those robots into the boundary of their target tiles.
- Phase (5) Local tile reconfiguration:** Locally reconfigure all tiles of the resulting tiled configuration.
- Phase (6) Scaffold deconstruction:** Reverse of Phase (2).

In the remainder of this section we provide details of the different phases. We start by providing some preliminaries needed for the detailed descriptions.

4.2 Preliminaries for the algorithm

In the following we give definitions that are fundamental for the understanding of the algorithm. We give additional definitions in each section as needed.

As an intermediate result for the labeled case, Demaine et al. [12] proposed an algorithm that computes schedules with stretch factors that are linear in the dimensions of a fully occupied rectangular area that is to be reconfigured.

► **Lemma 5.** *Let C_s and C_t be two labeled configurations of an $n_1 \times n_2$ rectangle with $n_1 > n_2 \geq 2$. There is a schedule $C_s \Rightarrow_{\chi} C_t$ with makespan $O(n_1 + n_2)$.*

In a follow-up paper, Fekete et al. [19] considered arbitrary unlabeled configurations, computing stable schedules of constant stretch. Note that stretch in the unlabeled case is defined via a bottleneck matching of robots between the start and target configuration. They make use of so-called *tilings*, *neighborhoods* of tiles, *layers* in tiles, a *scaffold* based on these layers, and *tiled configurations*, which we define as follows.

An m -tiling is a subdivision of a configuration's underlying grid into squares (called *tiles*) of side length $m \in \mathbb{N}$, each of them anchored at coordinates that are multiples of m in both dimensions. With scale c , diameter d , and $m = cd$, we refer to this tiling as \mathcal{T}_1 . For a tiling \mathcal{T} and a subset of tiles $\mathcal{T}' \subseteq \mathcal{T}$, the k -neighborhood $N_k[\mathcal{T}']$ is the set of all tiles from \mathcal{T} with Chebyshev distance at most k to any tile $T \in \mathcal{T}'$. The *boundary* of a tile consists of all nodes in the underlying grid graph that are immediately adjacent to its edge. The first *layer* of the tile is then the set of inward neighboring nodes of the boundary. This relationship applies to successive higher-order layers as well. The *scaffold* of a tiling is the union of all boundaries of its tiles. A *tiled configuration* is a configuration that is a subset of the given tiling and a superset of its scaffold. The *interior* of a tiled configuration is the set of all robots not part of the scaffold.

As an intermediate result they showed the following.

► **Lemma 6.** *Let C_s and C_t be two tiled unlabeled configurations such that C_s and C_t contain the same number of robots in the interior of each tile T . There is a schedule $C_s \Rightarrow_{\chi} C_t$ with makespan $O(d)$.*

4.3 Subroutine: Single tile reconfiguration

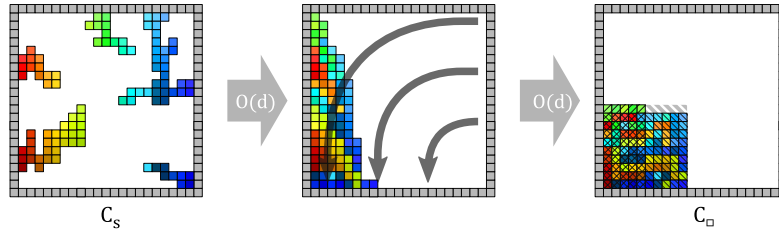
A key insight for our approach is that we can efficiently exploit a globally connected structure locally. Before explaining how we achieve this global structure, we show how to exploit it locally. This provides a fundamental subroutine that is used to locally transform tiled configurations within a makespan of $O(d)$. In particular, we obtain the following.

► **Theorem 7.** *For any two tiled connected configurations C_s and C_t for which each tile consists of the same robots, there is a stable schedule of makespan $O(d)$ that transforms one into the other.*

In the remainder of this subsection we provide several lemmas that yield a proof of Theorem 7. To this end, we first show that the interior of a tile can be reconfigured arbitrarily, followed by a description of how this can be adapted to include the reconfiguration of the boundary, as well as arbitrary exchanges of robots between a tile's interior and its boundary.

4.3.1 Reconfiguring the interior

We start by showing how the interior of a tile can be transformed arbitrarily. As moves are reversible, proving that a canonical configuration is reachable is sufficient. In our case, this configuration will be a subset of a square, see Figure 4.



■ **Figure 4** The canonical square-like configuration C_{\square} in the interior of a tile.

► **Lemma 8.** *For any two connected configurations consisting of an immobile $m \times m$ boundary for $m \in O(d)$ and $k \leq (m - 2)^2$ interior robots, there is a stable schedule of makespan $O(d)$ that moves all interior robots into a subset of $\lceil \sqrt{k} \rceil \times \lceil \sqrt{k} \rceil$ positions.*

Proof. Applying Lemma 6, the $k \leq (m - 2)^2$ robots that occupy positions in the tile's interior may be moved into a $\lceil \sqrt{k} \rceil \times \lceil \sqrt{k} \rceil$ square. The exact silhouette of this configuration depends exclusively on the number of robots. This can be realized in $O(d)$ transformations. ◀

Due to the relationship of any two sequential square numbers, i.e., $x^2 - (x - 1)^2 = 2x - 1$, at most $2\lceil \sqrt{k} \rceil - 1$ nodes within the $\lceil \sqrt{k} \rceil \times \lceil \sqrt{k} \rceil$ square may end up unoccupied. We form the silhouette in a manner such that these robots are missing within the top two rows, from an arbitrary but fixed end, see Figure 4.

► **Lemma 9.** *Given $k \in [6, (m - 2)^2]$ robots arranged in a subset of a $\lceil \sqrt{k} \rceil \times \lceil \sqrt{k} \rceil$ square, the robots may be arbitrarily rearranged by a stable schedule of makespan $O(d)$.*

Proof. As the silhouette varies based on the number of robots, we distinguish the following two cases.

If the configuration is a fully occupied rectangle, we can apply Lemma 5 to this rectangle to rearrange the robots in $O(d)$.

Otherwise, we cover the occupied area into two rectangles of size $[1, \lceil\sqrt{k}\rceil] \times [\lceil\sqrt{k}\rceil - 1, \lceil\sqrt{k}\rceil]$ and $\lceil\sqrt{k}\rceil \times [\lceil\sqrt{k}\rceil - 2, \lceil\sqrt{k}\rceil]$, respectively (see C_{\square} in Figure 4), which we reorder by applying Lemma 5 multiple times as follows. First, we ensure that the robots for the incomplete top row are located in the base of the taller rectangle, by reordering the lower rectangle. Then a second application to the enclosing section ensures that the incomplete row is correctly configured. For the case of a 1-wide rectangle, the empty position next to the robot may be considered a “pseudo-robot” and the operation may be applied to the corresponding 2-wide area instead. Finally, a third repetition ensures that the lower rectangle is also correctly ordered. Overall, this yields a makespan of $O(d)$. ◀

Note that the cases $k \in [1, 5]$ are excluded from the above lemma, but trivial schedules utilizing the existence of the boundary may be determined allowing arbitrary permutation.

4.3.2 Exchange between interior and boundary

Now we describe exchanges of robots between interior and boundary of tiles.

► **Lemma 10.** *For any tiled configuration of $m \times m$ -tiles for $m \in O(d)$, it is possible to exchange any number of robots from each tile’s interior with its boundary in $O(d)$ steps.*

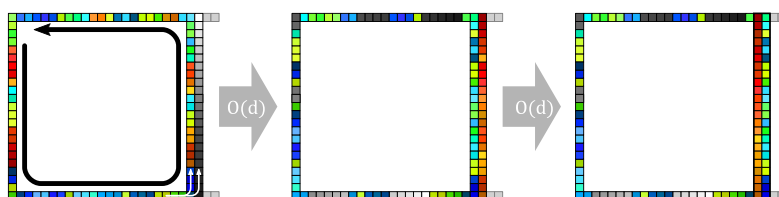
Proof. Place at most $4(m-4)$ robots that need to be swapped into the boundary, adjacent to the respective boundary robots that need to swap into the interior. Afterwards apply Lemma 5 to the disjoint areas in parallel. As there are fewer positions on a successive layer, we have to repeat this process at most once. As this operation is performed entirely within a single tile, it may be applied to all tiles simultaneously. ◀

4.3.3 Reconfiguring the boundary

It remains to show that the scaffolding structure can be reconfigured arbitrarily, without modifying its silhouette.

► **Lemma 11.** *The boundaries of all tiles within a tiled configuration that consists of $m \times m$ -tiles with $m \in O(d)$ may be locally reordered by a schedule of makespan $O(d)$.*

Proof. It is possible to arbitrarily reorder the boundary of a tile T in an $m \times m$ -tiled configuration without modifying the silhouette at all, provided an adjacent tile T' is not doing so at the same time. As the dual graph of the tiling is bipartite, the tiles can be partitioned into two disjoint sets, each of which can be reconfigured in parallel. This allows the $2 \times m$ area of boundary wall separating T and T' to be utilized as sorting space, as it is of suitable dimensions for application of Lemma 5. This means that an arrangement of $4m - 4 = O(d)$ robots along T ’s boundary may be reordered in $O(1)$ full revolutions around the tile’s interior.



■ **Figure 5** An illustration of the first iteration of the boundary reconfiguration approach.

By a full revolution of the boundary, we collect all m robots of a single side in the neighbor's portion of the sorting space, see Figure 5. By applying Lemma 5, this portion of the boundary can be rearranged. This sequence takes $O(d)$ steps. Afterwards, we can push the sorted m robots out of the sorting area and into the boundary, before “pre-sorting” the resulting selection of robots in the sorting area. Performing this process another $O(1)$ times on the remaining robots yields a sorted boundary. ◀

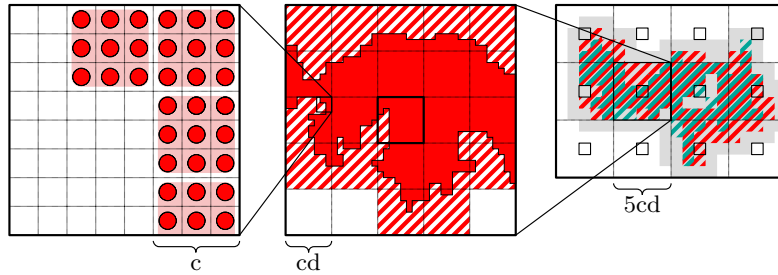
4.4 Phase (1): Preprocessing

Consider start and target configurations C_s and C_t . Let c refer to the minimum of the two configurations' scales and let d be the diameter of the pair (C_s, C_t) . Without loss of generality, assume that the configurations overlap in at least one position. Otherwise, we move the target configuration, such that it overlaps with the start configuration. This can be done in $O(d)$ steps, and results in a new diameter $d' \leq 2d$.

Using c and d , we define a cd -tiling \mathcal{T}_1 of the underlying grid. Let $\mathcal{T}_1(C_s)$ and $\mathcal{T}_1(C_t)$ refer to the set of tiles in \mathcal{T}_1 that contain robots in C_s and C_t , respectively (see red and green area in Figure 6). We observe that $N_1[\mathcal{T}_1(C_s) \cup \mathcal{T}_1(C_t)]$ is both a subset of $N_2[\mathcal{T}_1(C_s)]$ and of $N_2[\mathcal{T}_1(C_t)]$, because $\mathcal{T}_1(C_s)$ and $\mathcal{T}_1(C_t)$ are fully contained in each other's 1-neighborhoods.

Demaine et al. [12] exploited an $O(d)$ -tiling to guarantee that every robot's target position is either within its starting tile, or an immediate neighbor. In an extension of this approach, Fekete et al. [19] employed a cd -tiling; they constructed a scaffold along the tiling boundaries, achieving connectivity during the reconfiguration process. For configurations of sufficient scale, they drew robots from 2-neighborhoods in order to construct each tile's boundary. In our case, robots have individual target positions, so we must take their heading into account when constructing a scaffold. As a result, we consider a higher-resolution tiling, which allows us to ensure that the diameter of the instance does not increase due to scaffold construction.

Based on the non-empty tiles in \mathcal{T}_1 , we compute the higher-resolution cover of the relevant area by a grid of 5×5 squares of cd -tiles, see Figure 6. Let T_1, \dots, T_n be n tiles of \mathcal{T}_1 , such that the distance between any two of them is a multiple of 5 on both the x - and y -axis, and $N_1[\mathcal{T}_1(C_s) \cup \mathcal{T}_1(C_t)] \subseteq N_2[T_1] \cup \dots \cup N_2[T_n]$. We define the tiling $\mathcal{T}_5 := \{N_2[T_1], \dots, N_2[T_n]\}$.



■ **Figure 6** We derive a cd -tiling \mathcal{T}_1 (center) from the scale c (left) and the diameter of the instance. We then cover the neighborhood (right, in gray) of non-empty start and target tiles (dashed red and green, respectively) of \mathcal{T}_1 by a larger tiling \mathcal{T}_5 around which we construct a scaffold for stability.

This concludes the theoretical foundation of our approach. We will now proceed with the first transformation phase, which constructs the fundamental scaffold.

4.5 Phase (2): Scaffold construction

Having determined a cover of C_s and C_t in shape of the $5cd$ -tiling \mathcal{T}_5 , a scaffold spanning this cover is to be constructed. For this purpose, a robot is placed at every boundary position in \mathcal{T}_5 , which requires $(5 \cdot 4cd - 4)$ robots per tile. We show that there are sufficiently many robots to build the scaffold. For this, we refer to the *locally available material* for a given tile $T \in \mathcal{T}_5$ as the set of robots contained within T itself and its immediate neighborhood $N_1[T]$ over \mathcal{T}_5 .

► **Lemma 12.** *There is a constant c , such that for all C_s and C_t with scale at least c , there is sufficient locally available material to construct a boundary around all tiles of \mathcal{T}_5 .*

As \mathcal{T}_5 is a cover of $N_1[\mathcal{T}_1(C_s) \cup \mathcal{T}_1(C_t)]$, every tile $T \in \mathcal{T}_5$ contains at least one $T' \in N_2[\mathcal{T}_1(C_s)]$. We can thus guarantee sufficient locally available material for the boundary of T if we can show that it exists in the 4-neighborhood of any such T' .

To achieve this, we distinguish *donor* and *recipient* tiles. A donor tile contains enough robots to construct a boundary around itself and all eight immediate neighbors – any tile that cannot do this will be referred to as a recipient.

Proof of Lemma 12. Unless $cd \in \Omega(\sqrt{n})$, we can assume that both the start and target configurations consist of more than one tile in \mathcal{T}_1 ; otherwise, the reconfiguration problem is trivial. Without loss of generality, we thus assume that for any given non-empty tile $T \in \mathcal{T}_1$, there exist robots outside of its 1-neighborhood in C_s . This implies the existence of a path of length at least cd that connects T to those robots. Such a path has to be contained in a union of fully occupied pixels of size $c \times c$ due to the scale of both configurations. We can employ a proof by Fekete et al. [19] to derive that at least one neighbor of T must contain no less than $(c^2d)/4$ robots for $c \geq 4$.

Because \mathcal{T}_5 is a cover of the 2-neighborhood of non-empty tiles over \mathcal{T}_1 , we extend the above finding to conclude that every tile in \mathcal{T}_5 , or one of its neighbors, contains at least $(c^2d)/4$ robots.

We additionally note that the respective robots are located within the 4-neighborhood of each recipient tile over \mathcal{T}_1 . This is of particular relevance as these robots will remain within the 1-neighborhood over \mathcal{T}_5 for any target configuration.

A worst-case scenario has a tile donating to all eight of its neighbors, so it must contain at least $9(5 \cdot 4cd - 4)$ robots. We can guarantee sufficient material based on the above relationship, starting from a lower bound of $(c^2d)/4 \geq 9(20cd - 4) \Leftrightarrow c \geq 720$. ◀

► **Observation 13.** *Lemma 12 directly implies that every tile of \mathcal{T}_5 is either a donor, or an immediate neighbor of an applicable donor.*

The scaffold construction takes place in the following three subphases.

Phase (2.1): Parallel construction of all donor boundaries.

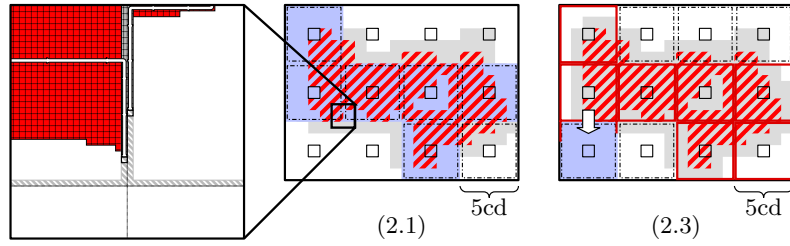
Phase (2.2): Mapping recipients to donors appropriately.

Phase (2.3): Construction of recipient boundaries.

► **Lemma 14.** *Each phase takes no more than $O(d)$ transformations.*

We now provide a brief overview of each phase.

For *Phase (2.1)*, consider a donor tile $T \in \mathcal{T}_5$. As each donor's interior contains enough robots to build its own scaffold, we can employ a very simple strategy to construct the boundaries. Within any such tile, we assign every robot a priority based on the length of the

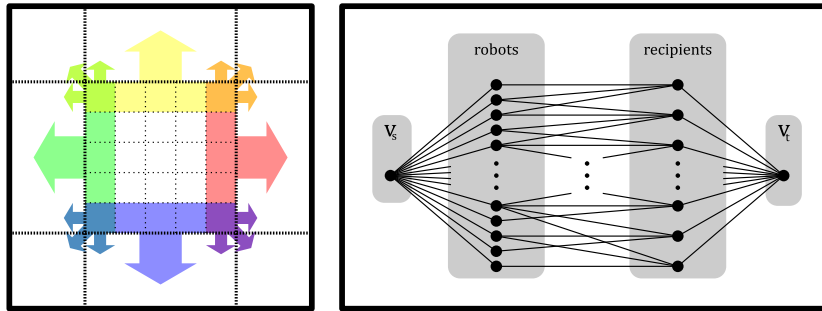


■ **Figure 7** The first and final subphases of scaffold construction visualized. Tiles with ongoing scaffold construction are highlighted in blue, while dashed boundaries indicate the state of the scaffold after each phase's termination.

shortest path in C_s that connects the robot to another robot that is adjacent to an empty position on the scaffold. Until T 's boundary is fully occupied, we repeatedly push along the respective shortest path of a robot with maximal priority in T , adding one robot to the scaffold structure (see also Figure 3 (2)). This approach does not cause disconnections in the configuration, as has been shown for the unlabeled problem variant [19]. Because the scaffold consists of $20cd - 4$ robots per tile, Phase (2.1) completes after $O(d)$ steps.

We already know that an applicable donor exists for each recipient tile (see Lemma 12), so *Phase (2.2)* simply focuses on determining an exact mapping between donors and recipients, while ensuring that the correct material is distributed in the final subphase. We achieve this by solving a flow problem over the dual graph of \mathcal{T}_5 before applying Theorem 7 to assemble specific robots from a donor for each recipient, again taking $O(d)$ transformations.

We model the necessary assignment of robots from donors to recipients as a flow network with source vertex v_s and sink vertex v_t . A maximal flow in this network can be decomposed into a set of (augmenting) paths that connect one robot from a donor tile to one adjacent recipient tile. This means that each path has the form (v_s, r, R, v_t) , with r being a robot currently located in a donor tile $D \in \mathcal{T}_5$ and a recipient tile $R \in \mathcal{T}_5$. All edges of type (v_s, r) or (r, R) have capacity one. Conversely, every edge (R, v_t) has capacity $20cd - 4$, see Figure 8.



■ **Figure 8** Robots within each \mathcal{T}_1 -tile in a \mathcal{T}_5 -tile T may have to leave T in different directions (left). We connect each robot to neighbors of T in a flow-graph (right) if and only if the neighbor does not lie opposite of its target tile.

Because we know that there is a sufficient number of robots in each recipient tile's vicinity, we know that a maximal flow fully utilizes all edges that connect recipients to the sink vertex v_t . The selection of edges between robots and recipients thus determines an applicable assignment of material.

As the construction scheme that we used before relies solely on the silhouette of a donating tile, we can easily determine to which adjacent recipient a robot at any given position in a donor tile will be sent. This includes scaffold locations near the boundary between two tiles that may have been occupied by robots with target neighbors opposite to the recipient tile. To account for this, we make use of Theorem 7 to assign the correct robots for each neighbor to the respective positions.

Phase (2.3) can then safely proceed to push robots from a donor tile into the boundary of adjacent recipients, using a variant of the method from Phase (2.1). We consider $3 \cdot 3$ classes of tiles, based on each tile's anchor position modulo $15cd$ and construct the boundaries of all recipient tiles in a class in parallel. For the movement of each robot, we map robots from the interior of a donor cell to a vertex on the respective recipient's boundary. Based on the previously discussed priority, robots are now pushed along their boundary and onto boundary vertices of the adjacent recipient. Once this process terminates, we have constructed a scaffold structure around all tiles of the cover \mathcal{T}_5 . This takes $20cd - 4$ transformations per tile class, so we conclude that Lemma 14 holds.

With the help of this global scaffold structure, connectivity is ensured during the actual reconfiguration. It remains to show how we shift robots between tiles, and reconfigure robot arrangements within the constructed scaffold. The latter has been already described in Section 4.3, so we describe how to relocate robots between tiles. This is modeled as a supply-demand flow for interior robots in three subphases:

Phase (3.1): Interior flow computation.

Phase (3.2): Interior flow partition.

Phase (3.3): Interior flow realization.

A similar approach is used to model the flow for boundary robots, see Section 4.9. We give descriptions of the different phases, and start with *Phase (3.1): Interior flow computation*.

4.6 Phase (3.1): Interior flow computation

Given any tile $T \in \mathcal{T}_5$, its interior robots either need to stay within it or move into a neighboring tile. The anticipated motion is represented as a supply-demand flow $G_{\mathcal{T}_5} := (\mathcal{T}_5, E_{\mathcal{T}_5}, f_{\mathcal{T}_5})$ of the dual graph of \mathcal{T}_5 . The flow value of an edge $f_{\mathcal{T}_5}(e)$ corresponds to the cardinality of the set of robots that need to move from one tile into another. A tile $T \in \mathcal{T}_5$ is a *source* (*sink*) if and only if the sum of flow values of incoming edges is smaller (larger) than the sum of flow values of outgoing edges. Otherwise, we call T *flow-conserving*. The difference of weights is called *supply* and *demand* for sources and sinks, respectively. If the flow value of every edge within a given flow graph is bounded from above by some value k , we refer to it as a *k-flow*. For simplicity, we consider the number of robots in the flow model, rather than the specific robots themselves.

► **Observation 15.** *The flow value $f_{\mathcal{T}_5}(e)$ of each edge $e \in E_{\mathcal{T}_5}$ is bounded from above by the interior space of the tiles, as each may contain at most $(5cd - 2)^2 < 25c^2d^2$ robots.*

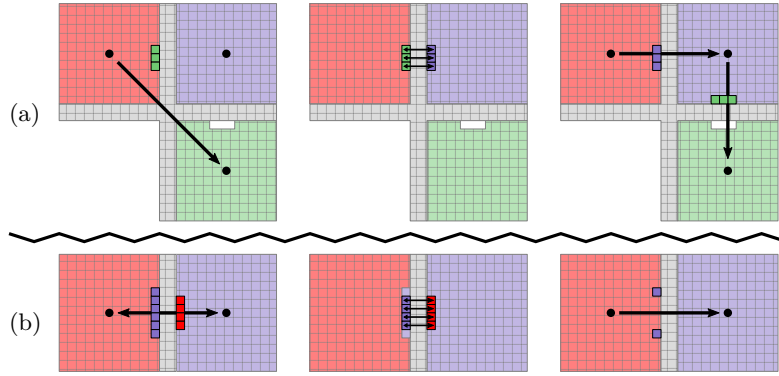
We say that a schedule *realizes* a flow graph $G_{\mathcal{T}_5} = (\mathcal{T}_5, E_{\mathcal{T}_5}, f_{\mathcal{T}_5})$ if for each pair $v, w \in \mathcal{T}_5$ of tiles, the number of robots moved by it from their start tile v to their target tile w is $f_{\mathcal{T}_5}((v, w))$, where we let $f_{\mathcal{T}_5}((v, w)) = 0$ if $(v, w) \notin E_{\mathcal{T}_5}$. Additionally, we define an (a, b) -*partition* of a flow graph as a set that contains b many a -flows that sum up to the original flow. By construction, the realization of a flow like the one above never requires us to fill a tile over capacity or to remove robots from an empty tile, as this would imply an invalid start or target configuration.

► **Lemma 16.** *It is possible to efficiently compute a stable schedule of makespan $O(d)$ that realizes $G_{\mathcal{T}_5}$.*

In the remainder of this section we provide an overview of the properties of $G_{\mathcal{T}_5}$ along with a detailed description of additional measures that split the graph into an acyclic and another totally cyclic component. For each of these components, we will provide an algorithm which computes a $(d, O(d))$ -partition of it. Finally, we discuss a set of unified movement patterns that realize each such flow partition through a schedule of makespan $O(d)$.

4.6.1 Creating a planar, unidirectional flow

As the initial flow graph may contain diagonal, bidirectional, or crossing edges, our first measure is to modify our initial tiled configuration such that the flow graph $G_{\mathcal{T}_5}$ becomes a planar, unidirectional graph, see Figure 9 for the underlying idea. Note that this process may triple the maximum flow value over every edge, resulting in a $3(5cd - 2)^2$ -flow.



■ **Figure 9** Preprocessing steps act on $G_{\mathcal{T}_5}$.

4.6.2 Removing diagonal edges, see Figure 9(a).

Similar to [12], crossing edges can only occur between two diagonal edges of adjacent source tiles $u, v \in G_{\mathcal{T}_5}$. To remove such a crossing, it suffices to eliminate one of the two edges by exchanging robots between u and v . Let w be a common neighbor of u and v , and consider without loss of generality that there is a diagonal edge (u, w) that has to be eliminated. For this, we simply exchange robots between the source tiles u, v in such a way that the flow $f_{\mathcal{T}_5}((u, w))$ is rerouted through v . For this, we exchange the robots in the interior of u that want to end up in w with robots of v that either want to stay in v or has their goal location in w , too.

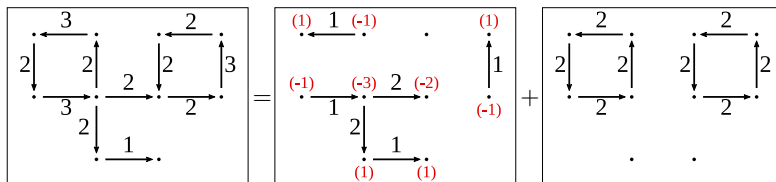
This increases the flow on the edges (u, v) and (v, w) by at most $(5cd - 2)^2$. Because there are only two possible tiles that are diagonal adjacent to v and adjacent to w , this can occur only two times. Note that by removing diagonal edges, no new diagonal edge can occur. After removing all crossing edges, we obtain $G_{\mathcal{T}}$ to be a $3(5cd - 2)^2$ -flow.

4.6.3 Removing bidirectional edges, see Figure 9(b).

Again, similar to [12], a bidirectional edge between two adjacent tiles $u, v \in G_{\mathcal{T}_5}$ can be removed by exchanging robots between u and v that want to switch to the other tile until one of the edges disappears.

4.7 Phase (3.2): Interior flow partition

$G_{\mathcal{T}_5}$ is now a planar graph, but neither guaranteed to be acyclic nor totally cyclic. Thus, the algorithm partitions $G_{\mathcal{T}_5}$ into two flows G_{\rightarrow} and G_{\circlearrowleft} , one being acyclic and the other totally cyclic, see Figure 10.



■ **Figure 10** An example decomposition of a flow graph into its acyclic and circular components.

► **Lemma 17.** *It is possible to efficiently compute a partition of $G_{\mathcal{T}_5}$ into an acyclic component G_{\rightarrow} and a totally cyclic component G_{\circlearrowleft} .*

This is a standard result from the theory of network flows; e.g., see Theorem 8.8 in Korte and Vygen [25] or the book by Ford and Fulkerson [21].

4.7.1 Partitioning the circular flow

For the case of configurations that do not have to be connected, Demaine et al. [12] considered tiles of side length $24d$. Thus, they obtained a totally cyclic flow graph G_{\circlearrowleft} with an upper bound of $24d \cdot 24d = 576d^2$ for the flow value of each edge. Furthermore, they showed that it is possible to compute a $(d, O(d))$ -partition of G_{\circlearrowleft} . In our case, we have to keep configurations connected, resulting in tiles of side length cd . Thus, we extend the peeling algorithm from [12], resulting in a specific flow partition to a more general version.

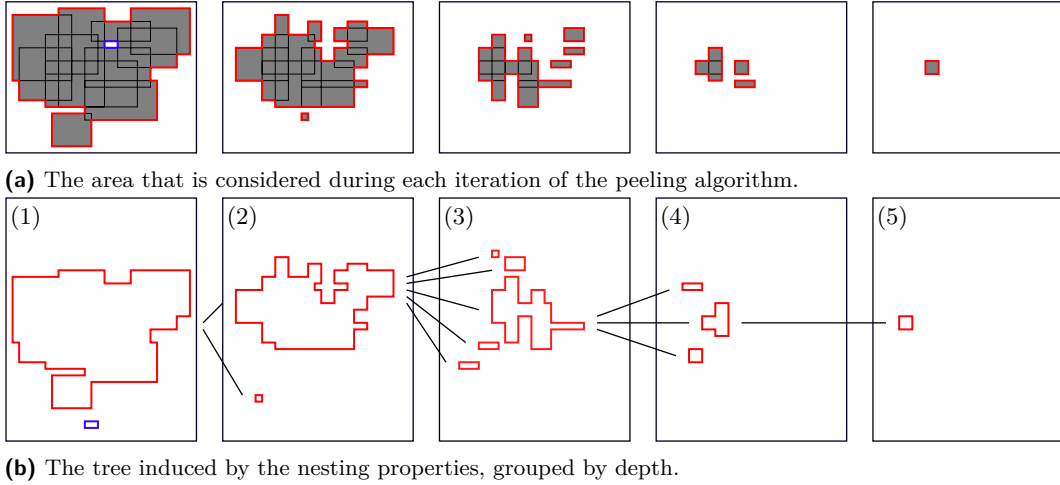
► **Lemma 18.** *A $(d, O(d))$ -partition of the totally cyclic $k \cdot d^2$ -flow G_{\circlearrowleft} for $k \in \mathbb{N}$ into totally cyclic flows can be computed efficiently.*

Proof. Consider a tiled configuration C' of scale c and let n denote the total number of robots. The following steps yield a $(d, O(d))$ -partition of G_{\circlearrowleft} .

Starting with *Step (1)*, we compute a $(1, h)$ -partition $\mathbb{P}_{\circlearrowleft}$ of G_{\circlearrowleft} . The number of flows h is bounded from above by the total number of robots n , as each robot may only contribute to a single cycle. If any cycle intersects itself, it is subdivided into smaller, non-intersecting cycles. Afterwards, $\mathbb{P}_{\circlearrowleft}$ can be divided into two classes of cycles based on cycle orientation. Let $\mathbb{P}_{\circlearrowright}$ refer to the clockwise cycles and $\mathbb{P}_{\circlearrowleft}$ to the counterclockwise cycles of $\mathbb{P}_{\circlearrowleft}$.

In *Step (2)*, we compute a $(1, h)$ -partition using the sets $\mathbb{P}_{\circlearrowright}$ and $\mathbb{P}_{\circlearrowleft}$. The resulting subsets $\mathbb{P}_{\circlearrowright}^1 \cup \mathbb{P}_{\circlearrowright}^2 \cup \mathbb{P}_{\circlearrowleft}^1 \cup \mathbb{P}_{\circlearrowleft}^2$ are constructed in a fashion such that two cycles u and v from the same subset share the same orientation and are either edge-disjoint or nested within another, where we write $u \sqsubseteq v$ if v contains u .

Such a partition may be constructed using a geometric peeling algorithm such as the one devised by Demaine et al. [12], see Figure 11. Their approach handles each $\mathbb{P}_X \in \{\mathbb{P}_{\circlearrowright}, \mathbb{P}_{\circlearrowleft}\}$ separately. Considering the union of inner-bound areas A of all cycles in \mathbb{P}_X , a 1-circulation around the outer edges of each component of A is identified, removed from \mathbb{P}_X and added to the set \mathbb{P}_X^1 . Simultaneously, inversely oriented 1-circulations around any holes within A are removed from \mathbb{P}_X , and added to the set \mathbb{P}_X^2 (see Figure 11(a)). This process is repeated until \mathbb{P}_X is fully decomposed into the two sets $\mathbb{P}_X^1, \mathbb{P}_X^2$.



■ **Figure 11** Iterations of the peeling algorithm. The outer loops that go into a set \mathbb{P}_X^1 are marked red and the inner boundary loops of set \mathbb{P}_X^2 are marked in blue.

In the final *Step (3)*, each $\mathbb{P}_X^j \in \{\mathbb{P}_\circ^1, \mathbb{P}_\circ^2, \mathbb{P}_\circ^1, \mathbb{P}_\circ^2\}$ will now be partitioned into $O(d)$ sets that form one d -subflow of G_\circ each.

As previously noted, any pair of cycles in \mathbb{P}_X^j is either edge-disjoint, or one of the cycles lies within the other. This property induces a forest $F = (\mathbb{P}_X^j, E_F)$ in which one cycle u is a child of another cycle v exactly if $u \sqsubseteq v$ and there is no other cycle w such that $u \sqsubseteq w \sqsubseteq v$ (see Figure 11(b)).

Given such a forest, every vertex is labeled by its depth in $F \bmod kd$. These labels are then used to construct $O(d)$ subflows $\{G_{\circ_1}, G_{\circ_2}, \dots\}$, each G_{\circ_i} being the union of cycles with label i .

▷ **Claim.** Every flow G_{\circ_i} constructed by this algorithm is a d -subflow of G_\circ .

Consider any $u, v \in \mathbb{P}_X^j$ such that the two cycles share a common edge e . By construction, one of the two cycles must lie within the other, so without loss of generality, assume that $u \sqsubseteq v$. This implies that there exists a path from u to its root via v in F , with all cycles on the path between u and v sharing the edge e as well. As G_\circ has all edges bounded from above by $k \cdot d^2$, the cycles containing e lie on a path of length no more than $k \cdot d^2$ in F . Thus, e has a weight of at most $(k \cdot d^2)/(k \cdot d) = d$ in every G_{\circ_i} , meaning G_{\circ_i} is a d -flow. ◀

Applying the above algorithm to G_\circ yields a (d, ℓ) -partition for $\ell < 75c^2 \cdot d = O(d)$. As the elements of such a partition of G_\circ add up to G_\circ itself, its realization may now be reduced to the realization of all d -subflows.

4.7.2 Partitioning the acyclic flow

In the previous section, we computed a $(d, O(d))$ -partition of G_\circ . As $G_\circ + G_\rightarrow = G_{\tau_5}$, we still need to compute a $(d, O(d))$ -partition of G_\rightarrow to obtain a $(d, O(d))$ -partition of the entire flow G_{τ_5} . In the context of unlabeled robots, Fekete et al. [19] proposed an algorithm for computing a $(O(d^2), 28)$ -partition of G_\rightarrow . Due to the much more complex situation of labeled robots, we employ a number of more refined ideas to provide an algorithm that guarantees the following.

► **Lemma 19.** *A $(d, O(d))$ -partition of the acyclic $k \cdot d^2$ -flow G_{\rightarrow} for $k \in \mathbb{N}$ into acyclic flows can be computed efficiently.*

Proof. It is possible to compute a partition of $G_{\rightarrow} = (\mathcal{T}_5, E, f_{\vec{T}})$ into 1-subflows, each being a path that connects a supply vertex to a demand vertex, simply by performing a decomposition of the flow. As G_{\rightarrow} is both planar and unidirectional, this means it may be viewed as a directed forest, with each component A containing a subset of the paths. The following process is then applied to each tree $A \subseteq G_{\rightarrow}$ separately.

First, an arbitrary vertex of A is chosen as root of the component. For any path P_i in A , its *link distance* refers to the minimal length of any path connecting a vertex of P_i to the root of A . Consider (P_1, P_2, \dots) as sorted by link distance. Every path P_i is now greedily assigned to a set S_j , such that the first edge e_1 of P_i is not part of any other path in S_j . These sets are shared over the components of G_{\rightarrow} , and if no matching set exists for a path P_i , a new set $S_j := \{P_i\}$ is created. As the maximum incoming degree of the head vertex of a directed edge is three in the setting of a grid graph, each edge of the graph may be contained in at most three paths of each set.

Once these sets are fully constructed, they are greedily partitioned into groups of $d/3$ sets $\{G_{\rightarrow_1}, G_{\rightarrow_2}, \dots\}$. For each group G_{\rightarrow_i} , a subflow f_i is created that maps an edge to the number of paths in G_{\rightarrow_i} that contain it. Because every edge can appear no more than three times within a set of paths S_j and each group contains $d/3$ sets, each f_i is a $(d/3 \cdot 3) = d$ -subflow of G_{\rightarrow} .

▷ **Claim.** The constructed partition $(G_{\rightarrow_1}, G_{\rightarrow_2}, \dots)$ contains at most $75c^2d = O(d)$ subflows.

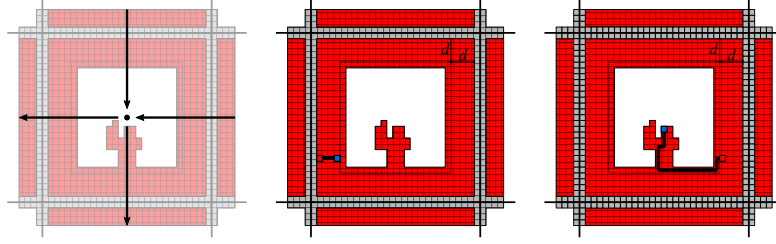
As $G_{\mathcal{T}_5}$ is initially bounded from above by the interior space of a tile, the substitution of diagonal edges leaves G_{\rightarrow} bounded below $3(5cd - 2)^2$. Suppose the previously described approach constructs $75c^2d$ flows. This implies that the algorithm encountered a state with $\lambda = 75c^2d \cdot d/3 - 1$ existing sets S_1, \dots, S_λ and the current path P_i had to be assigned to a new set $S_{\lambda+1}$. We conclude that each set S_1, \dots, S_λ contained a path P_j that included the first edge e_1 of P_i , meaning that there were at least $75c^2d \cdot d = 3(5cd)^2 > 3(5cd - 2)^2$ paths that contained e_1 , which contradicts our premise. ◀

4.8 Phase (3.3): Interior flow realization

In order to exchange robots between tiles as modeled by the flow $G_{\mathcal{T}_5}$, we have to determine a collision-free protocol that allows robots to pass through the scaffold and into adjacent tiles. To this end, we describe a set of movement patterns for the robots of a single tile; these realize a single d -subflow in a stable manner within $O(d)$ steps. To achieve a compact concatenation of these movement patterns, an invariant type of local tile configuration is of significant importance. Using this invariant, we then provide more compact movement patterns that realize up to d such d -subflows via a schedule of makespan $O(d)$.

These invariant configuration of a tile $T \in \mathcal{T}_5$ are *push-stable* (with respect to a flow $G_{\mathcal{T}_5}$), defined by the following connectivity conditions for every robot r on an i th layer of the interior of T .

- $i \leq d$: r is connected to the closest boundary robot by a straight line of robots.
- $i > d$: r is connected to a robot r' on layer d by a path of robots in higher-order layers than d , such that the closest side to r' of the boundary of T rests on an edge without outgoing flow.



■ **Figure 12** An example of a push-stable configuration of a tile with two incoming and two outgoing edges (left). Highlighted are a robot on layer d (center) and on a higher-order layer (right), with paths that ensure their connectivity.

A *total sink* (*total source*) is a tile T that has four incoming (outgoing) edges of non-zero value over $G_{\mathcal{T}_5}$. Conversely, a *partial sink* (*partial source*) is a tile T that is not flow-conserving over $G_{\mathcal{T}_5}$, but has no more than three incoming (outgoing) edges of non-zero value. Note that by definition, total sources can never be configured in a push-stable manner. As a consequence, we handle both total sinks and total sources separately, as described in Section 4.8.3.

4.8.1 Realizing a single subflow

We now provide the detailed description of our approach to realize a single subflow. The approach consists of the following three subphases.

Phase (3.3.A): Interior preprocessing.

Phase (3.3.B): Matching incoming and outgoing robots.

Phase (3.3.C): Pushing robots into their target tiles.

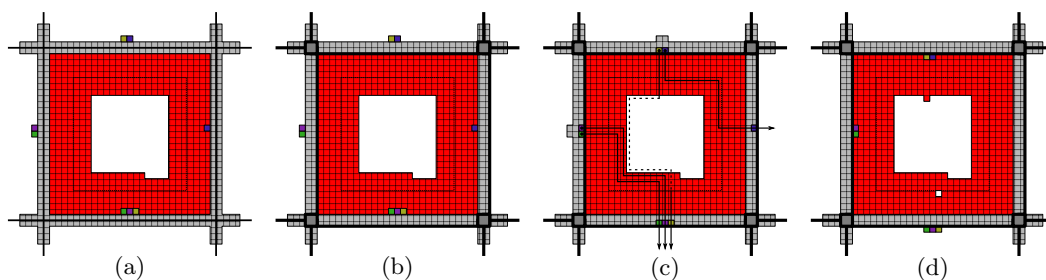
► **Lemma 20.** *Consider a d -subflow $H_{\mathcal{T}_5} \subseteq G_{\mathcal{T}_5}$ and a tile $T \in \mathcal{T}_5$ that is flow-conserving with respect to $H_{\mathcal{T}_5}$. There is a schedule of makespan $O(d)$ that realizes the flow at its location.*

Using Theorem 7, *Phase (3.3.A)* constructs a push-stable initial configuration that places $0 < d' \leq d$ outgoing robots adjacent to their respective target tile’s shared boundary in the interior of T .

Afterwards, a local application of Lemma 5 is used to embed those outgoing robots into the boundary between their current and target tile, allowing them to be pushed into the interior of a neighboring tile in a single step, see Figure 13(c).

For simplified notation, parts of the scaffold are temporarily “reassigned” to neighboring tiles for this purpose. For instance, a tile T may temporarily surrender ownership of its half of the scaffold separating it from a neighboring tile T' , see Figure 13(b), assuming $f'((T', T)) > 0$. The 2×2 corner areas are never reassigned.

In *Phase (3.3.B)*, we perform a pairwise matching of incoming and outgoing robots, so that each pair can be connected by a crossing-free path. Each such path passes through a unique layer $d + i$ for some $i \in \mathbb{N}$, depending on the matching, meaning that some paths might pass through incomplete or missing layers (see Figure 13(c)). Note that any such path begins adjacent to a robot that enters T , travels inwards to the $(d + i)$ th layer, at which point follows said layer until it travels outwards again to the boundary of T , reaching the vertex at which the matched robot leaves T . This approach closely follows the methods described by Demaine et al. [12] in their paper on a related reconfiguration problem.



■ **Figure 13** A tile $T \in \mathcal{T}_5$ during the realization of a single d -subflow. The dashed portions of paths indicate that no motion actually occurs in this segment due to the described pushing behavior.

The actual realization of $H_{\mathcal{T}_5}$ at tile T can now be performed in a single, simultaneous pushing motion along each of the constructed paths in *Phase (3.3.C)*, see Figure 13(d).

► **Lemma 21.** *The realization of a d -subflow can be performed in a way that results in another push-stable configuration of T .*

Proof. The crucial steps for this occur in *Phase (3.3.C)*. Consider a path that connects an incoming and an outgoing robot. If the path is fully occupied, the described pushing motion does not have any effect on the silhouette of the tile it passes through, so this motion by itself yields a push-stable configuration.

Now consider a path through an incomplete layer that has an incoming robot entering it at the first position. We continue the resulting pushing motion until the first empty position on the path, which then becomes occupied.

The tail end of the path is handled differently. The last d positions on the path may be occupied by robots that are then always connected directly to the scaffold through one another. We push only these (at most) d robots towards the boundary, potentially leaving a hole at the d th layer of the tile, see Figure 13(d). Note that the positions immediately before the last d may be occupied by robots as well. However, any robot above layer d must be connected to an *incoming* side of the boundary via a path through its own layer. This ensures that any robot above the d th layer remains connected regardless of the outgoing robots moving away from it.

We conclude that *Phase (3.3.C)* always results in a push-stable configuration. ◀

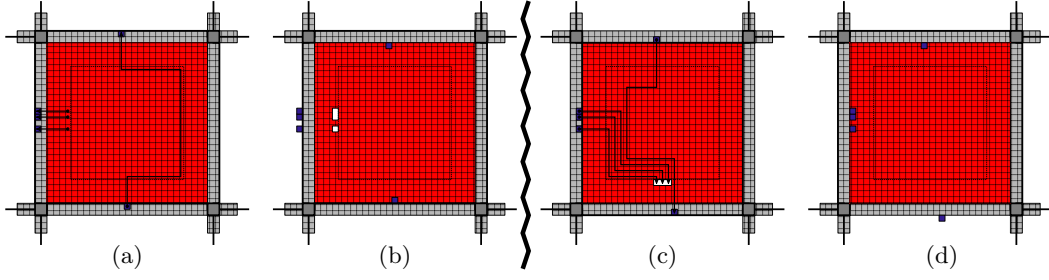
We slightly modify the above approach, in order to apply it to non-flow-conserving tiles.

► **Lemma 22.** *Consider a d -subflow $H_{\mathcal{T}_5} \subseteq G_{\mathcal{T}_5}$ and a tile $T \in \mathcal{T}_5$ that is not a total sink or total source with respect to $G_{\mathcal{T}_5}$. There is a schedule of makespan $O(d)$ that realizes the flow at its location and yields another push-stable configuration.*

Proof. Consider a tile T that is not flow-conserving with respect to a d -subflow $H_{\mathcal{T}_5}$ and for which there are $\lambda \leq d$ robots either entering or leaving the tile that cannot be matched to a robot doing the opposite. See Figure 14 for an illustration.

If T is a partial source, a push-stable initial configuration may be created by the previously outlined method. As the pulling motion at the outgoing end of a path always results in another push-stable configuration, the lack of incoming robots does not cause any disconnections.

If T is a partial sink, a slight adjustment to the initial push-stable configuration must be made. As $\lambda \leq d$, it is possible to leave λ empty positions in the d th layer, behind outgoing robots. The result is a push-stable configuration that allows the incoming paths to push into the empty space behind the outgoing robots, reaching another push-stable configuration. ◀



■ **Figure 14** A partial source tile (left) and a partial sink tile (right) during the realization of a single d -subflow

4.8.2 Realizing multiple subflows

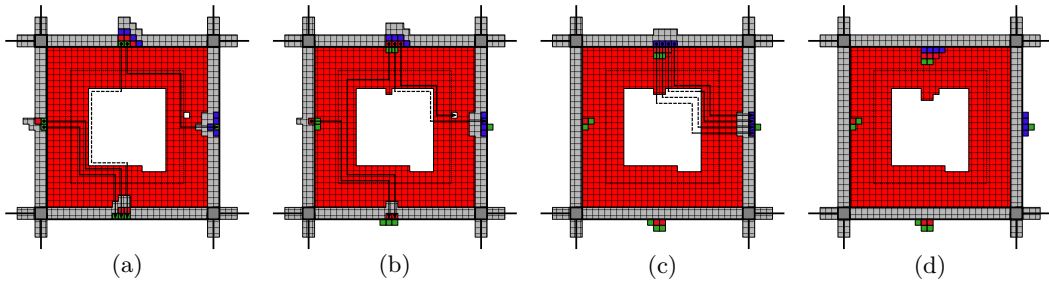
The previously described movement patterns may be compactly combined into a single schedule of makespan $O(d)$ that realizes up to d many d -subflows at once.

► **Lemma 23.** *Consider a tile $T \in \mathcal{T}_5$ that is not a total sink or total source with respect to $G_{\mathcal{T}_5}$ and a sequence $S_{\mathcal{T}_5} := (H_{\mathcal{T}_5}^1, \dots, H_{\mathcal{T}_5}^\ell)$ of d -subflows of $G_{\mathcal{T}_5}$ with $\ell \leq d$. There exists a stable schedule of makespan $O(d)$ that realizes all ℓ many d -subflows.*

Proof. The first portion of this schedule consists of an application of Theorem 7 that prepares for the final ℓ transformation steps that realize one subflow each, see Figure 15. This is achieved by stacking the robots against the target tile's boundary in successive layers, for which the order of robots is based on the order of subflows in $S_{\mathcal{T}_5}$, with later subflows occupying locations on higher-order layers. As $\ell \leq d$, no queue may be more than d robots long. The result is a push-stable configuration of T , which takes into account the special cases discussed in Lemma 22.

Next, we apply Theorem 7 to embed the queues of robots in the wall between their current and their target tile, placing corresponding scaffold robots at the very back of each queue, see Figure 15(a). This leaves only the actual realization steps to be determined.

These consist of ℓ successive pushing operations based on matchings between incoming and outgoing robots, ensuring that each intermittent configuration of the schedule is stable. ◀



■ **Figure 15** A tile $T \in \mathcal{T}_5$ during the realization of ℓ d -subflows.

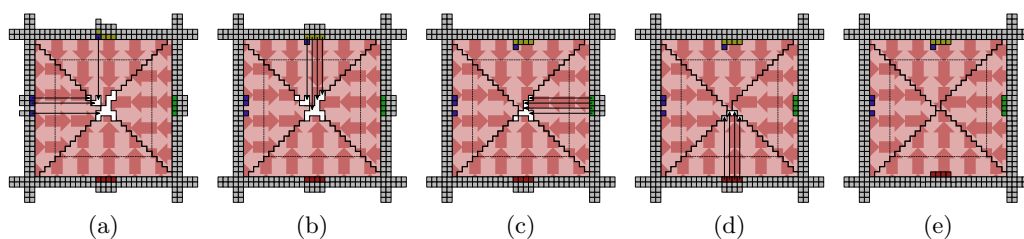
4.8.3 Total sinks and sources

As noted before, total sinks and sources form a special case that we handle separately from the described push-stable patterns.

► **Lemma 24.** Consider a tile $T \in \mathcal{T}_5$ that is a total sink or total source with respect to $G_{\mathcal{T}_5}$ and a sequence $S_{\mathcal{T}_5} := (H_{\mathcal{T}_5}^1, \dots, H_{\mathcal{T}_5}^\ell)$ of d -subflows of $G_{\mathcal{T}_5}$ with $\ell \leq d$. There exists a stable schedule of makespan $O(d)$ that realizes all ℓ many d -subflows.

Proof. We divide the interior space of T into four disjoint triangles along the diagonals of the tile, see Figure 16. Without loss of generality, assume that T is a total sink. No more than d^2 robots can enter at any given edge as a result of $S_{\mathcal{T}_5}$ and the resulting number of robots in the tile's interior cannot be more than $(5cd - 2)^2$. This means that it is sufficient to leave the corresponding number of positions at the innermost section of each triangle unoccupied. The motion of entering robots cannot cause any issues with stability and takes no more than ℓ transformations. This implies a total makespan of $O(d) + \ell$.

As every schedule is invertible, the opposite movement pattern may be applied to total sources; pushing outwards from the very center of the tile while only moving robots within a single triangle region does not cause any disconnections of the configuration. ◀



■ **Figure 16** A total sink $T \in \mathcal{T}_5$ during the realization of ℓ many d -subflows. As indicated by the triangular marks, each side has a unique space into which robots may push.

4.8.4 Realizing all subflows

By applying Lemmas 23 and 24, up to d many d -subflows of $G_{\mathcal{T}_5}$ may be realized in $O(d)$ transformations. As we created $O(d)$ such subflows in Section 4.7, all of them may be realized through $O(d)/d = O(1)$ repetitions. These repetitions require a total of $O(d)$ transformations.

4.9 Phase (4): Boundary flow

The next phase of our algorithm deals with the movement of robots that are part of the scaffold. As described in Section 4.5, the robots forming the scaffold in a tiled configuration must remain in the 1-neighborhood of their target tile over \mathcal{T}_5 . The intermediate mapping step in the construction process guarantees that this remains the case even after that phase concludes. However, the scaffold does not necessarily consist of the same robots in the tiled configurations C'_s and C'_t .

► **Observation 25.** For any given tile $T \in \mathcal{T}_5$, up to $20cd - 4$ robots exist in its neighborhood $N_1[T]$ that need to become part of its boundary structure.

This observation induces another supply-demand flow graph similar to the one in Section 4.6, with each edge's flow value bounded from above by $20cd - 4$. Using the techniques discussed in Sections 4.6 and 4.7, we obtain a $(d, O(1))$ -partition of this flow graph. This requires minor modifications to the involved methods.

4.9.1 Creating a planar and unidirectional flow

Just as with the prior flow $G_{\mathcal{T}_5}$, bidirectional and diagonal edges need to be removed from the flow before the partitioning process. This can be achieved in the same manner as before. Applying Theorem 7, we place the robots that we need to exchange between adjacent tiles in the wall between them, before exchanging them by means of local rotations. As at most $20cd - 4$ robots need to be swapped between any two tiles, this process takes $O(d)$ steps total. Once this process has been applied to all tiles, G_s is bounded from above by $3(20cd - 4)$.

4.9.2 Partitioning the flow

As the flow G_s is bounded from above by the number of robots on each tile's boundary, it will be broken down into smaller components that can be realized separately. A $(d, O(1))$ -partition can be computed via the following method.

By applying Lemma 17, we compute a $(3(20cd - 4), 2)$ -partition of G_s , decomposing the flow into circular and acyclic components G_{\rightarrow}^s and G_{\circlearrowleft}^s . Using modified versions of the previously introduced partitioning algorithms, we compute a $(d, O(1))$ -partition of each.

► **Lemma 26.** *By modifying the final step of the algorithm for Lemma 18, we can compute a $(d, O(1))$ -partition of a circulation G_{\circlearrowleft} which is a $k \cdot d$ -flow for some constant $k \in \mathbb{N}$ in polynomial time.*

Proof. See Lemma 18 for the first two steps of the algorithm. Let $\mathbb{P}_X^j \in \{\mathbb{P}_{\circlearrowleft}^1, \mathbb{P}_{\circlearrowleft}^2, \mathbb{P}_{\circlearrowright}^1, \mathbb{P}_{\circlearrowright}^2\}$ refer to a partition constructed in Step (2). Additionally, let $F = (\mathbb{P}_X^j, E_F)$ refer to the forest induced by the nesting properties of cycles within the partitions.

Labeling the vertices of this forest by their depth in $F \bmod k$, it is possible to construct $O(1)$ subflows $\{G_{\circlearrowleft 1}, G_{\circlearrowleft 2}, \dots\}$, each being the union of cycles sharing a label.

▷ **Claim.** Each subflow $G_{\circlearrowleft i}$ with $i \in [1, k]$ is a d -subflow.

Consider any two cycles $u, v \in \mathbb{P}_X^j$ that share a common edge e . By construction, one of the two cycles must lie within the other. Without loss of generality, assume that v lies in u . This implies that there exists a path from v to its root via u in F , with all cycles on the path between v and u sharing the edge e as well. As all edges in G_{\circlearrowleft} are bounded from above by $k \cdot d$, the cycles containing e lie on a path of length no more than $k \cdot d$ in F . Thus, e has a weight of at most $k \cdot d / k = d$ in every $G_{\circlearrowleft i}$. We conclude that $G_{\circlearrowleft i}$ is a d -subflow of G_{\circlearrowleft} . ◀

We now compute a $(d, O(1))$ -partition of G_{\rightarrow}^s .

► **Lemma 27.** *Applying the algorithm for Lemma 19 to an acyclic flow G_{\rightarrow} which is a $k \cdot d$ -flow for some constant $k \in \mathbb{N}$ yields a $(d, O(1))$ -partition of G_{\rightarrow} .*

Proof. See the proof of Lemma 19 for the algorithm itself. We know that G_{\rightarrow} is bounded from above by $k \cdot d$. Suppose the algorithm constructs $k + 1$ flows, implying that the algorithm encountered a configuration in which a path P_i could not be assigned to the existing $\lambda = 3k \cdot d/3$ sets S_1, \dots, S_{λ} , spawning a new set $S_{\lambda+1}$. This implies that each set S_1, \dots, S_{λ} contained a path P_j that shares the first edge e_1 of P_i , meaning that there were at least $k \cdot d + 1 > k \cdot d$ paths containing e_1 , implying a flow value of more than $k \cdot d$. ◀

4.9.3 Realizing a single subflow

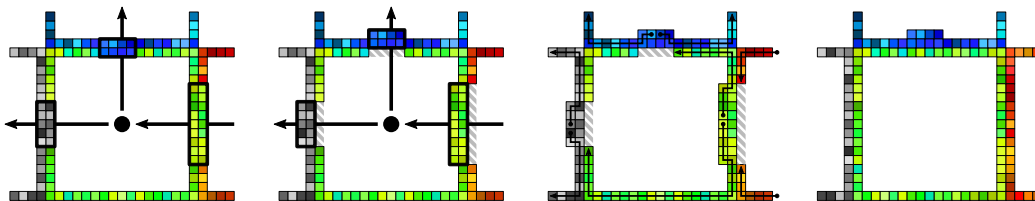
► **Lemma 28.** *Let $H_s = (\mathcal{T}_5, E_{\mathcal{T}_5}, f_s^l)$ be a d -subflow of G_s . We can efficiently compute a schedule of makespan $O(d)$ that realizes H_s .*

Proof. The exact movement comes down to the number of robots within each tile the flow passes through.

Consider any tile $T \in \mathcal{T}_5$ that has non-zero flow in H_s and let $\Gamma \leq (5cd)^2$ be the initial number of robots within the tile (including the scaffold). Additionally, let $\Gamma_{\text{out}} \leq d$ denote the exact number of robots that need to leave T to realize H_s at its location. Each tile always contains at least its boundary robots, so $\Gamma \geq 20cd - 4$. The existing movement patterns from Section 4.8 may be utilized to realize the flow at T 's location if $\Gamma - \Gamma_{\text{out}} \geq 20cd - 4$.

On the other hand, if $\Gamma - \Gamma_{\text{out}} < 20cd - 4$, there are not sufficiently many robots within the tile's interior to close up the holes in the scaffold through which the Γ_{out} robots leave it as part of the pushing motion. Note that this can only occur at flow-conserving tiles, because source tiles cannot end up with less robots than $20cd - 4$. This means that there are $\Gamma_{\text{in}} = \Gamma_{\text{out}}$ robots entering T as part of the same flow.

As every outgoing side of T is adjacent to an incoming side of another tile T' , no part of the scaffold can become disconnected through the pushing motion. Afterwards, there are at most Γ_{in} unoccupied positions in the boundary of T . By pushing along and into the boundary from the middle of the line of Γ_{in} robots that were pushed into T , those robots may patch all holes in $O(\Gamma_{\text{in}}) = O(d)$ transformations (see Figure 17). Overall, this shows that it is possible to realize a single d -subflow of G_s in $O(d)$ steps. ◀



■ **Figure 17** We can employ the displayed movement patterns to exchange boundary robots between adjacent tiles.

4.9.4 Realizing all subflows

► **Lemma 29.** *We can compute a schedule of makespan $O(d)$ that realizes G_s , transforming a tiled configuration C'_s into another tiled configuration C'_t for C_s and C_t with diameter d , in polynomial time.*

Proof. The entirety of G_s may be realized by applying the previous approach to each of the d -subflows computed in Section 4.9.2, bringing all scaffold robots into their correct target tiles. As there are $O(1)$ such subflows, the total makespan of this step is $O(d)$. ◀

4.10 Phase (5): Local tile reconfiguration

Once Phase (4) concludes, we have reached a tiled configuration in which every tile contains precisely the robots that it would in a tiled configuration C'_t of the target configuration. This means that we can reconfigure into C'_t by a single application of Theorem 7, which forms the entirety of Phase (5).

As Phase (6) is a reverse of Phase (2), this concludes the description of the algorithm. Because each phase takes $O(d)$ transformation steps, this proves Theorem 4.

4.11 Decentralized methods

Besides the robot motion itself, there are two additional aspects of parallelization: distributed methods for (1) carrying out computations and (2) performing motion control. Both issues can be addressed to some extent by making use of the hierarchical structure of our approach, which operates on (I) the macroscopic tile graph, as well as on (II) the set of robots within tiles. Making use of the canonical algorithmic structures and reconfigurations within tiles, it is relatively straightforward to do this at the individual tile levels (II) based on local operations (for computation) and protocols (for motion control). The macroscopic aspects (I) can be addressed by making use of distributed methods for computing network flows, such as [23]; using these in our context requires embedding the high-level flow graph into the scaffold framework and implementing the corresponding distributed algorithms as protocols into our lower-level scaffold structures.

5 Conclusion and future work

We provided new results for efficient coordinated motion planning for a labeled swarm of robots. In particular, we resolved two major open problems for connected reconfiguration: in the labeled case, a stretch factor of $\Omega(n)$ may be inevitable for n robots, and constant stretch can be achieved for scaled arrangements of labeled robots; previously, the former was unknown for any kind of connected reconfiguration, while the latter was only known for the (considerably easier) unlabeled case.

Some open problems remain. We believe that it is possible to provide a tight upper bound on the stretch factor for general (not necessarily scaled) arrangements: any connected arrangement of n robots and arrangement diameter $D \leq n$ allows a makespan of $O(\sqrt{D})$. Additional questions arise from reducing the involved constants, as well as further practical methods (along the lines of the recent CG Challenge as well as practical robotics). Of interest are also implementations of largely distributed computation and motion control for efficient parallel motion schedules, as sketched in Section 4.11.

All these challenges are left for future work.

References

- 1 Aviv Adler, Mark de Berg, Dan Halperin, and Kiril Solovey. Efficient multi-robot motion planning for unlabeled discs in simple polygons. *IEEE Transactions on Automation Science and Engineering*, 12(4):1309–1317, 2015. doi:10.1109/TASE.2015.2470096.
- 2 Hugo A. Akitaya, Esther M. Arkin, Mirela Damian, Erik D. Demaine, Vida Dujmovic, Robin Y. Flatland, Matias Korman, Belén Palop, Irene Parada, André van Renssen, and Vera Sacristán. Universal reconfiguration of facet-connected modular robots by pivots: The $O(1)$ musketeers. *Algorithmica*, 83(5):1316–1351, 2021. doi:10.1007/s00453-020-00784-6.
- 3 Hugo A. Akitaya, Erik D. Demaine, Matias Korman, Irina Kostitsyna, Irene Parada, Willem Sonke, Bettina Speckmann, Ryuhei Uehara, and Jules Wolms. Compacting squares: Input-sensitive in-place reconfiguration of sliding squares. In *Scandinavian Symposium and Workshops on Algorithm Theory (SWAT)*, pages 4:1–4:19, 2022. doi:10.4230/LIPIcs.SWAT.2022.4.
- 4 Aaron T. Becker, Sándor P. Fekete, Phillip Keldenich, Matthias Konitzny, Lillian Lin, and Christian Scheffer. Coordinated motion planning: The video. In *Symposium on Computational Geometry (SoCG)*, pages 74:1–74:6, 2018. Video at <https://www.ibr.cs.tu-bs.de/users/fekete/Videos/CoordinatedMotionPlanning.mp4>. doi:10.4230/LIPIcs.SoCG.2018.74.
- 5 Julien Bourgeois, Sándor P. Fekete, Ramin Kosfeld, Peter Kramer, Benoît Piranda, Christian Rieck, and Christian Scheffer. Space ants: Episode II - coordinating connected catoms. In

- Symposium on Computational Geometry (SoCG)*, pages 65:1–65:6, 2022. doi:10.4230/LIPIcs.SoCG.2022.65.
- 6 Gruia Călinescu, Adrian Dumitrescu, and János Pach. Reconfigurations in graphs and grids. *SIAM Journal on Discrete Mathematics*, 22(1):124–138, 2008. doi:10.1137/060652063.
 - 7 Soon-Jo Chung, Aditya Avinash Paranjape, Philip Dames, Shaojie Shen, and Vijay Kumar. A survey on aerial swarm robotics. *IEEE Transactions on Robotics*, 34(4):837–855, 2018. doi:10.1109/TR0.2018.2857475.
 - 8 Loïc Crombez, Guilherme Dias da Fonseca, Yan Gerard, Aldo Gonzalez-Lorenzo, Pascal Lafourcade, and Luc Libralesso. Shadoks approach to low-makespan coordinated motion planning. In *Symposium on Computational Geometry (SoCG)*, pages 63:1–63:9, 2021. doi:10.4230/LIPIcs.SoCG.2021.63.
 - 9 Mark de Berg and Amirali Khosravi. Optimal binary space partitions for segments in the plane. *International Journal on Computational Geometry and Applications*, 22(3):187–206, 2012. doi:10.1142/S0218195912500045.
 - 10 Daniel Delahaye, Stéphane Puechmorel, Panagiotis Tsiotras, and Eric Féron. Mathematical models for aircraft trajectory design: A survey. In *Air Traffic Management and Systems*, pages 205–247. Springer, 2014. doi:10.1007/978-4-431-54475-3_12.
 - 11 Erik D. Demaine, Martin L. Demaine, Sándor P. Fekete, Mashhood Ishaque, Eynat Rafalin, Robert T. Schweller, and Diane Souvaine. Staged self-assembly: Nanomanufacture of arbitrary shapes with $O(1)$ glues. *Natural Computing*, 7(3):347–370, 2008. doi:10.1007/s11047-008-9073-0.
 - 12 Erik D. Demaine, Sándor P. Fekete, Phillip Keldenich, Christian Scheffer, and Henk Meijer. Coordinated motion planning: Reconfiguring a swarm of labeled robots with bounded stretch. *SIAM Journal on Computing*, 48(6):1727–1762, 2019. doi:10.1137/18M1194341.
 - 13 Erik D. Demaine, Sándor P. Fekete, Christian Scheffer, and Arne Schmidt. New geometric algorithms for fully connected staged self-assembly. *Theoretical Computer Science*, 671:4–18, 2017. doi:10.1016/j.tcs.2016.11.020.
 - 14 Erik D. Demaine, Matthew J. Patitz, Robert T. Schweller, and Scott M. Summers. Self-assembly of arbitrary shapes using RNase enzymes: Meeting the Kolmogorov bound with small scale factor. In *Symposium on Theoretical Aspects of Computer Science (STACS)*, pages 201–212, 2011. doi:10.4230/LIPIcs.STACS.2011.201.
 - 15 Adrian Dumitrescu and János Pach. Pushing squares around. *Graphs and Combinatorics*, 22(1):37–50, 2006. doi:10.1007/s00373-005-0640-1.
 - 16 Adrian Dumitrescu, Ichiro Suzuki, and Masafumi Yamashita. Formations for fast locomotion of metamorphic robotic systems. *International Journal of Robotics Research*, 23(6):583–593, 2004. doi:10.1177/0278364904039652.
 - 17 Adrian Dumitrescu, Ichiro Suzuki, and Masafumi Yamashita. Motion planning for metamorphic systems: feasibility, decidability, and distributed reconfiguration. *IEEE Transactions on Robotics*, 20(3):409–418, 2004. doi:10.1109/TRA.2004.824936.
 - 18 Sándor P. Fekete, Björn Hendriks, Christopher Tessars, Axel Wegener, Horst Hellbrück, Stefan Fischer, and Sebastian Ebers. Methods for improving the flow of traffic. In *Organic Computing — A Paradigm Shift for Complex Systems*. Springer, 2011. doi:10.1007/978-3-0348-0130-0_29.
 - 19 Sándor P. Fekete, Phillip Keldenich, Ramin Kosfeld, Christian Rieck, and Christian Scheffer. Connected coordinated motion planning with bounded stretch. In *International Symposium on Algorithms and Computation (ISAAC)*, pages 9:1–9:16, 2021. doi:10.4230/LIPIcs.ISAAC.2021.9.
 - 20 Sándor P. Fekete, Phillip Keldenich, Dominik Krupke, and Joseph S. B. Mitchell. Computing coordinated motion plans for robot swarms: The CG:SHOP Challenge 2021, 2021. arXiv:2103.15381.
 - 21 Lester R. Ford and Delbert R. Fulkerson. *Flows in networks*. Princeton University Press, 1962.

- 22 Seth C. Goldstein and Todd C. Mowry. Claytronics: A scalable basis for future robots. 2004. URL: <http://www.cs.cmu.edu/~claytronics/papers/goldstein-robosphere04.pdf>.
- 23 Zhipeng Jiang, Xiaodong Hu, and Suixiang Gao. A parallel Ford-Fulkerson algorithm for maximum flow problem. In *International Conference on Parallel and Distributed Processing Techniques and Applications (PDPTA)*, pages 71–74, 2013.
- 24 Stephen Kloder and Seth Hutchinson. Path planning for permutation-invariant multi-robot formations. *IEEE Transactions on Robotics and Automation*, 22(4):650–665, 2006. doi:10.1109/TR0.2006.878952.
- 25 Bernhard H. Korte and Jens Vygen. *Combinatorial optimization*. Springer, 2011.
- 26 Paul Liu, Jack Spalding-Jamieson, Brandon Zhang, and Da Wei Zheng. Coordinated motion planning through randomized k-opt. In *Symposium on Computational Geometry (SoCG)*, pages 64:1–64:8, 2021. doi:10.4230/LIPIcs.SoCG.2021.64.
- 27 Austin Luchsinger, Robert T. Schweller, and Tim Wylie. Self-assembly of shapes at constant scale using repulsive forces. *Natural Computing*, 18(1):93–105, 2019. doi:10.1007/s11047-018-9707-9.
- 28 Michael Rubenstein, Alejandro Cornejo, and Radhika Nagpal. Programmable self-assembly in a thousand-robot swarm. *Science*, 345(6198):795–799, 2014. doi:10.1126/science.1254295.
- 29 Erol Şahin and Alan F. T. Winfield. Special issue on swarm robotics. *Swarm Intelligence*, 2(2-4):69–72, 2008. doi:10.1007/s11721-008-0020-6.
- 30 Michael Schreckenberg and Reinhard Selten. *Human Behaviour and Traffic Networks*. Springer, 2013. doi:10.1007/978-3-662-07809-9.
- 31 Jacob T. Schwartz and Micha Sharir. On the piano movers’ problem: III. Coordinating the motion of several independent bodies: the special case of circular bodies moving amidst polygonal barriers. *International Journal of Robotics Research*, 2(3):46–75, 1983. doi:10.1177/027836498300200304.
- 32 David Soloveichik and Erik Winfree. Complexity of self-assembled shapes. *SIAM Journal on Computing*, 36(6):1544–1569, 2007. doi:10.1137/S0097539704446712.
- 33 Kiril Solovey and Dan Halperin. k -color multi-robot motion planning. *International Journal of Robotics Research*, 33(1):82–97, 2014. doi:10.1177/0278364913506268.
- 34 Kiril Solovey and Dan Halperin. On the hardness of unlabeled multi-robot motion planning. *International Journal of Robotics Research*, 35(14):1750–1759, 2016. doi:10.1177/0278364916672311.
- 35 Kiril Solovey, Jingjin Yu, Or Zamir, and Dan Halperin. Motion planning for unlabeled discs with optimality guarantees. In *Robotics: Science and Systems*, 2015. doi:10.15607/RSS.2015.XI.011.
- 36 Matthew Turpin, Nathan Michael, and Vijay Kumar. Trajectory planning and assignment in multirobot systems. In *Algorithmic Foundations of Robotics X - Workshop on the Algorithmic Foundations of Robotics (WAFR)*, pages 175–190. Springer, 2013. doi:10.1007/978-3-642-36279-8_11.
- 37 Matthew Turpin, Kartik Mohta, Nathan Michael, and Vijay Kumar. Goal assignment and trajectory planning for large teams of interchangeable robots. *Autonomous Robots*, 37(4):401–415, 2014. doi:10.1007/s10514-014-9412-1.
- 38 Hyeyun Yang and Antoine Vigneron. A simulated annealing approach to coordinated motion planning. In *Symposium on Computational Geometry (SoCG)*, pages 65:1–65:9, 2021. doi:10.4230/LIPIcs.SoCG.2021.65.